

Fabrication and electrical characterization of Organic Field-Effect Transistor based on CSA doped PANi-Ta₂O₅ nanocomposite

Bornali Bora Patowary¹, Shakuntala Laskar²,
Rewrewa Narzary³

¹Department of Electronics and Communication Engineering,
Central Institute of Technology, BTAD, Kokrajhar, Assam - 783370

bb.patowary@cit.ac.in

²Department of Electrical and Electronics Engineering, School of Technology, Assam Don
Bosco University, Azara, Guwahati, Assam – 781017
shakuntalalaskar@gmail.com

³Department of Electronics and Communication Engineering, Tezpur University, Napam,
Assam – 784028
rewa325@gmail.com

Keywords: Organic field-effect transistor (OFET), CSA-PANi-Ta₂O₅, gate dielectric, long channel, charge carrier mobility.

(Article history: Received: 28th February 2020 and accepted 28th June 2020)

Abstract—Top-contact, bottom-gate organic field-effect transistors (OFETs) based on Polyaniline (PANi)-Tantalum Pentoxide (Ta₂O₅) nanocomposite doped with Camphor Sulphonic Acid (CSA) as the active semiconductor layer and Poly Methyl Methacrylate (PMMA) as the gate dielectric were investigated. Gold was thermally evaporated for the top source and drain contacts of 80-90 nm thickness with a conducting channel of 1 mm length and 1 cm width. A relatively good charge carrier mobility of 0.12 cm²/V-s was achieved. This may be ascribed to the highly crystalline nature of the nanocomposite, the diminished contact resistance due to the long channel and the symbiosis developed between the organic semiconductor and the polymer dielectric. The smaller source-to-drain current and high saturation drain voltage may be accounted for the long channel effect. The device exhibited a threshold voltage of -12.89 V, a moderate current on/off ratio of ~10³ and a subthreshold swing of 9.3 V/dec. The agglomerated globular morphology of the PANi nanocomposite and the high carrier mobility can immensely contribute towards using the OFET device for room-temperature based application, particularly in the gas sensing field.

I. Introduction

Organic electronic devices such as the organic field-effect transistors (OFETs) have emerged as the revolutionary technology towards the advent of new generation low cost, flexible electronics. OFETs based on conducting polymers (CPs) and their nanocomposites have established as a promising constituent in the field of large-area electronic displays, gas sensors [1], integrated optoelectronic devices, wearable devices [2], electronic skin and nose [3,4], implantable medical circuits [5], environmental monitoring devices [6] etc. This has motivated enormously the research fraternity to develop new materials based on organic semiconductors (OSCs), both CPs and small molecules of

immense potential to develop the active layer in the design of the OFETs. The performance of OFETs has shown dramatic improvements over the years in terms of charge carrier mobility, stability, low operating voltage and working temperature. Past works reported of pentacene based OFETs that achieved high carrier mobility from 0.3 up to 0.9 cm²/V-s [7]. Y.Y. Lin et al. [8] used double layers of pentacene in the OFET to obtain high carrier mobility of 1.5 cm²/V-s, current on/off ratio greater than 10⁸, threshold voltage almost zero and a sub-threshold swing as low as 1.6 V/dec. L.N. Ismail et al. [9] demonstrated poly (3-hexylthiophene-2,5-diyl) (P3HT) based p-type OFETs with poly methyl methacrylate (PMMA) and titanium dioxide (TiO₂) nanocomposite as the dielectric material that showed carrier mobility 2.01 cm²/V-s and threshold voltage -3V.

K. Kim and co-workers [10] fabricated single crystal rubrene based top-contact, p-type OFETs with spin coated poly (4-hydroxystyrene) as the gate dielectric and achieved carrier mobility of 1.12 cm²/V-s, threshold voltage of -0.3 V, current on/off ratio of 10² and 1.6 nA of leakage current. They showed that the device exhibited improved performance over the OFETs devised with the ceramic dielectric silicon nitride (Si₃N₄) in bottom contact configuration.

Y. Li et al. [11] fabricated CSA-PANi based OFET with the electrolyte poly(ethyleneimine) (PEI) inserted between the semiconductor layer and the gate dielectric polyvinyl pyrrolidone (PVP) and achieved carrier mobility of 2.48 12 cm²/V-s. They found that without the PEI, the device exhibited resistor behavior.

Over the several decades, conducting polymers (CPs) have witnessed growing importance owing to their intrinsic potentials such as structural diversity, tailor-made electrical/electronic properties, easy synthesis process and environmental stability [12]. These fascinating properties have made the CPs stand out in the crowd of the inorganic

competitors. In 1977, H. Shirakawa, A. MacDiarmid and A. Heeger made the revolutionary breakthrough into the discovery of polyacetylene. Since then, various important CPs such as polypyrrole (PPy), polyaniline (PANi), polythiophene (PT), poly(3,4-ethylenedioxythiophene) (PEDOT), and poly(p-phenylene vinylene) (PPV) have been investigated incessantly [13].

Conducting polymers (CPs) are polymers with conjugated backbone chain with alternating single and double (π) bonds along the chain. These π -conjugated systems render the CPs unique optical, electrochemical, and electrical/electronic (conductivity) properties. To achieve enhanced conductivity, the CPs are doped either through redox mechanism or protonation.

As stated above, the reasons behind the numerous research attentions on CPs today are their inherent properties of easy synthesis process, good mechanical and environmental stability and more importantly the ability to tailor their molecular structure and morphology as per the need [14]. CPs such as polyacetylene, polythiophene (PTh), polypyrrole (Ppy), polyaniline (PANi), poly(3,4- ethylenedioxythiophene (PEDOT) have been successfully used in various types of sensors such as chemiresistive thin-film gas sensors, OFETs, surface acoustic wave (SAW), optrode and amperometric sensors [15].

The category of nanocomposite made of CPs and inorganic material develops altogether a new set of properties that depends not only on their individual original properties but also on their interfacial characteristics. The material properties of such hybrid materials can be fine-tuned at the molecular level to achieve the desired result [16]. S. Huh et al. and B. Chae et al. [17,18] devised an innovative photo-patternable OFETs based on poly (3-hexylthiophene), gold nanoparticles and photoreactive cinnamate group. X. Chen et al. [19] reported a flexible low-voltage operated OFET based on cross-linked PVP blended with novel ceramic material calcium titanate nanoparticles as the gate dielectric. Several groups reported gas sensors based on such nanocomposites with promising results [20,21].

Among the CPs, PANi is one of the most commonly used material in OFETs due to its simple chemical structure, good environmental stability, easy synthesis process, interesting redox property, and relatively high conductivity [22]. In several past works, PANi has been used successfully in conjunction with nanoparticles of metal oxides as the active layer to achieve breakthrough particularly in the field of gas sensing [23-26].

The research of the gate dielectrics has found as importance as that of the OSCs to achieve high-performance OFETs. The desirable requirements of the gate dielectrics to be used in OFETs are high capacitance (for high drain current while operating at a lower voltage), solution processibility and compatibility with flexible substrates [27]. Inorganic dielectrics possess high dielectric constant but they offer a rough surface and it is difficult to cast them on a large surface. An organic dielectric makes a smooth surface and helps in the proper growth of the organic semiconductor surface [28]. A polymeric dielectric can operate at a low processing temperature, can lower the leakage current and the operating voltage [29,30], and facilitate a trap-free

semiconductor/dielectric interface enhancing the charge carrier mobility [31].

PMMA is a synthetic resist obtained from the polymerization of methyl methacrylate used in the high-resolution process of nanolithography that uses electron beam, UV or X-ray radiation. It has good thermal and mechanical stability, and a high resistivity greater than 10^{15} ohm-cm. PMMA has a permittivity of 2.6 at 1 MHz and a dielectric constant of 3.9 at 60 Hz. These make PMMA similar to silicon dioxide and hence it becomes suitable to be used as dielectric. Also, it is easier to deposit PMMA using spin-coating method and baked at low temperature [32].

J. Puigdollers [32] and coworkers devised a pentacene based OFET with PMMA as the gate dielectric and obtained carrier mobility of $0.01 \text{ cm}^2/\text{V-s}$ and threshold voltage of -15 V. These features are attributed to improved morphology of pentacene influenced by the underlying gate dielectric.

K. Amer et al. [33] demonstrated an effective humidity sensor based on PANi doped with dodecyl benzene sulphonic acid (DBSA) using PMMA as the gate dielectric.

A. Maliakal et al. [34] reported charge carrier mobility of $0.2 \text{ cm}^2/\text{V-s}$ approx. for a pentacene based OFET incorporating high-K $\text{TiO}_2/\text{polystyrene}$ nanostructure. Wang et al. [35] reported a flexible OFET based on silk fibroin as the gate dielectric to achieve high carrier mobility of $23.2 \text{ cm}^2/\text{V-s}$ and a low operating voltage of -3 V.

An OFET is consisted of three electrodes viz., source, drain and gate, a semiconductor layer as the active layer and an insulator layer as the gate dielectric that lies between the semiconductor layer and the gate (Fig. 1). A voltage is applied at the gate terminal to control the current flow between the source and the drain.

The most common variety of OFETs is the p-type OFETs because of the relatively high hole mobility of the OSC they employ and the ease of synthesis process of most of the p-type OSCs [36,37]. A negative voltage greater in magnitude than the threshold voltage of the OSC is applied between the gate and the source which causes a p-type channel to form at the OSC-gate dielectric interface. A negative drain-to-source voltage is also applied to cause the holes to flow from source to drain. The magnitude of the drain-to-source voltage is increased until the “pinch-off” condition takes place. At this point, the p-type channel converges close to one side and the drain current reaches its saturation. The magnitude of the saturation current depends on the gate-to-source voltage [38].

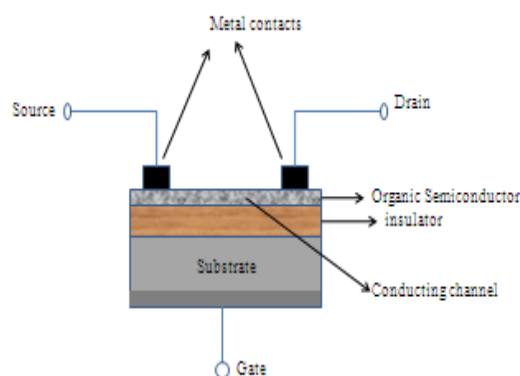


Fig.1. Device configuration of top-contact bottom-gate OFET.

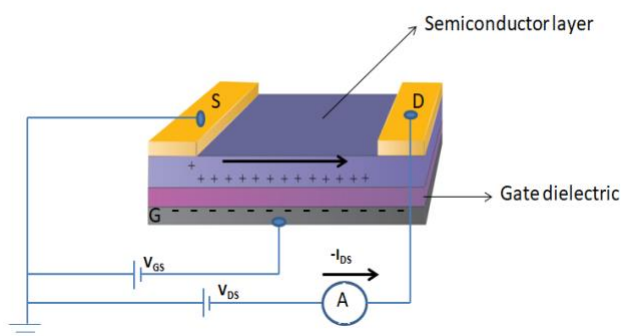


Fig.2. Device operation of p-type OFET with top contacts and bottom gate (both V_{DS} and V_{GS} are negative).

The schematic of the OFET operation for p-type conduction (hole conduction) is shown in Fig. 2. The desirable performance parameters of an OFET are high charge carrier mobility (μ) and current on/off ratio (I_{ON}/I_{OFF}), and low threshold voltage (V_{TH}) and sub-threshold swing (SS).

Previously, our group synthesized and studied the surface morphology and spectroscopic properties of PANi-Ta₂O₅ (50wt%) nanocomposite doped with CSA in 20wt%, 30wt% and 40wt% respectively [39]. The nanocomposite with CSA40wt% was found to exhibit good sensing behavior towards environmentally toxic gas NO₂.

In the current work, we fabricated a top-contact, bottom-gate OFET device based on PANi-Ta₂O₅ nanocomposite doped with CSA in 40wt% using PMMA as the gate dielectric. We, then, investigated the electrical characteristics of the OFET.

The novelty of our present work is based on using the acid doped PANi based organic-inorganic hybrid material which was used as the active layer of the OFET. Material characterization of the PANiTa₂O₅-CSA [39] revealed its potential in the gas sensing field.

The device under study was fabricated using a facile and cost effective fabrication process. It was possible to perform solution deposition of both the organic semiconductor and the polymer dielectric due to their good solubility. The deposition technique is a determining factor of OFET performance.

A relatively good performance of the device under study was achieved at room temperature. We found limited but promising works in the literature on OFETs based on CP based nanocomposite comprising of the polymer and inorganic counterparts [40-42]. Our future work is motivated in implementing the proposed device for gas sensing application.

II. Experimental

2.1. Material Preparation

The synthesis process and preparation of PANi-Ta₂O₅(50wt%) doped with CSA(40wt%) was reported in our previous work [39]. This nanocomposite was used as the active layer of the OFET device.

2.2 Material Characterization

The CSA doped PANi-Ta₂O₅ nanocomposite was analyzed through i) Scanning Electron Microscopy (using ZEISS SIGMA variable pressure field emission scanning electron microscope (FESEM)), ii) Fourier Transform Infrared (FTIR) spectroscopy using a Nicolet 6700 spectrometer over the wave number range of 4000-500 cm⁻¹ and iii) powder XRD analysis of the samples were recorded using X-ray diffraction (XRD, Brukers AXS, Germany/D8 Focus) with Cu-K α radiation, beam wavelength=1.54Å operated at 40KVA/40m within the 2 θ range of 5^o-85^o.

2.3. Fabrication process

ITO coated glass substrate (0.5 cm × 0.5 cm) was used for making the OFET device and the bottom gate electrode. Before initiating the fabrication process, the substrate was cleaned thoroughly using RCA1 followed by RCA2 and then dried at room temperature.

PMMA was obtained from free radical polymerization of methyl methacrylate and benzoyl peroxide as the initiator at room temperature. 10 mg of PMMA was diluted in 100 ml of anisole and the solution was spun on the ITO coated glass substrate at 800 rpm for 80 seconds. The PMMA layer was then dried in a conventional oven at 50°C for 1 hour. The thickness of the PMMA layer was measured with Spectroscopic Ellipsometer (Make : Semilab) and found to be ~500 nm.

PANi-Ta₂O₅-CSA nanocomposite was synthesized and produced in the form of fine powder. A good dispersion was obtained by dispersing the nanocomposite in NMP (N-methylpyrrolidine) in 10wt% and made it to stir on a magnetic stirrer for 4 hours. The nanocomposite was then deposited on the PMMA layer using spin-coating technique at 1000 rpm for 80 seconds. The deposited layer was then dried in an oven at 50°C for 1 hour.

Gold was used to make the top source and drain contacts. All the metal contacts, each with thickness 80-90 nm, were deposited using thermal evaporation with a hard mask in a physical thermal vacuum coating system (BC-300, Hind High Vacuum) maintaining the pressure at 2×10⁻⁵ Torr. The schematic of the OFET with channel length (L) 1 mm and channel width (W) 1 cm was shown in Fig.3.

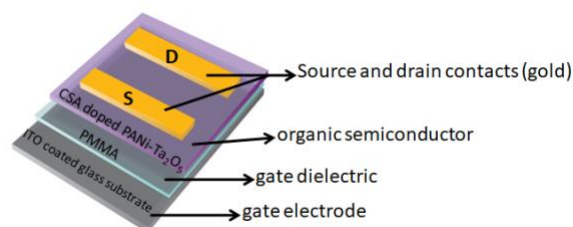


Fig. 3. Schematic of the proposed CSA doped PANi-Ta₂O₅ OFET device.

2.4 Electrical Characterization

The electrical characterization of the OFET device was

done under ambient condition at 25°C room temperature and 55% relative humidity using Keithly 2450 Sourceter and Keithly 6517 B electrometer/high-resistance meter. For the output characteristics, the gate was biased with a constant voltage (V_{GS}) and a voltage was applied between the drain and the source (V_{DS}), with the later being grounded. V_{DS} was swept through 0 V to -50V, while the corresponding value of I_{DS} was recorded. For each output plot, V_{GS} was kept fixed at 0 V though -50 V in steps of -10 V.

The quality of the OFET is mainly determined by the values of charge carrier mobility (μ), threshold voltage (V_{TH}), current on/off ratio and subthreshold swing (SS). These parameters were measured subsequently.

III. Results and discussion

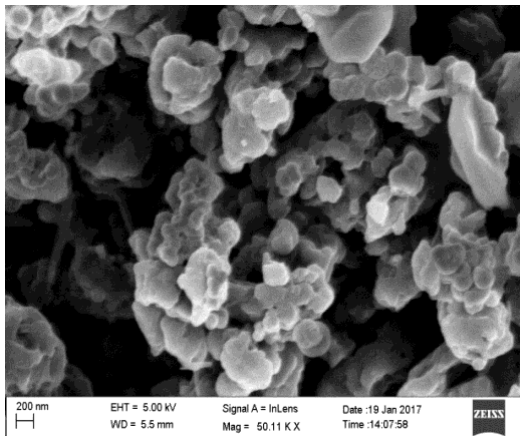


Fig. 4. FESEM image of PANi-Ta₂O₅-CSA nanocomposite [39].

Fig. 4 shows the FESEM micrograph of PANi-Ta₂O₅-CSA nanocomposite which revealed highly aggregated globular structures of ± 200 nm diameter. Studies [43] reveal that these PANi nanostructures can possess high conductivity and large surface area and become suitable for gas sensing applications.

Fig.5. shows the FTIR spectrum of PANi-Ta₂O₅-CSA nanocomposite. FTIR studies are known to be useful to identify the important chemical bonds and functional groups of a given material. In the spectra every wavelength of light absorbed characterizes a specific chemical bond.

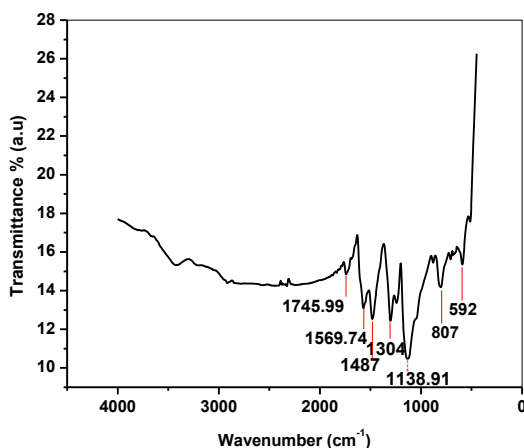


Fig. 5. FTIR spectrum of PANi-Ta₂O₅-CSA nanocomposite [39].

As seen in Fig.5, the peaks at 807 cm⁻¹ and 1138.91 cm⁻¹ may be responsible for the stretching vibration modes of O=Ta=O bonds. The peak at 1304 cm⁻¹ belongs to PANi-Ta₂O₅ molecule. The addition of CSA into PANi-Ta₂O₅ molecule resulted in the formation of peaks at 592 cm⁻¹, 1487 cm⁻¹, 1569.74 cm⁻¹ and 1745.99 cm⁻¹ and they are ascribed to =S=O bond for CSA.

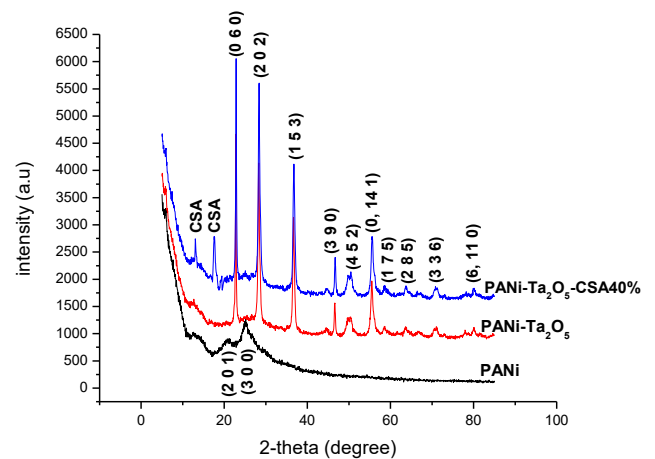


Fig. 6. XRD graphs of PANi, PANi-Ta₂O₅ and PANi-Ta₂O₅-CSA40% nanocomposite [39].

As seen in XRD graphs of Fig.6, pure PANi possessed two distinct peaks at $2\theta=20.68^\circ$ and at $2\theta=25.24^\circ$. This suggests the formation of PANi nanostructure that exists in semi-crystalline form. The XRD pattern of PANi-Ta₂O₅ confirms the presence of Ta₂O₅ in the nanocomposite. It is confirmed from the XRD graph that Ta₂O₅ retained its own crystal structure even being dispersed in the PANi matrix.

The XRD pattern of PANi-Ta₂O₅-CSA40wt% revealed two prominent peaks at $2\theta=13.04^\circ$ and $2\theta=17.58^\circ$ which are responsible for the presence of CSA molecule in the nanocomposite. Some other peaks of PANi-Ta₂O₅-CSA40% attained greater intensity with respect to those of PANi-Ta₂O₅. This confirms PANi-Ta₂O₅-CSA40% has greater crystallinity over PANi-Ta₂O₅ [39].

Fig. 6 depicts the output and transfer characteristics of CSA doped PANi-Ta₂O₅ OFET device.

The output characteristics shown in fig.6.a depict a high operating voltage which might have resulted due to the low-k PMMA dielectric [27]. The drain-to-source current, I_{DS} displays quadratic dependence on V_{GS} in saturation due to the long channel effect. Also, the saturation drain current at $V_{GS}=-50$ V seemed not so pronounced.

The key parameters of the OFET, viz. the charge carrier mobility (μ), threshold voltage (V_{TH}) and current on/off ratio were evaluated as follows.

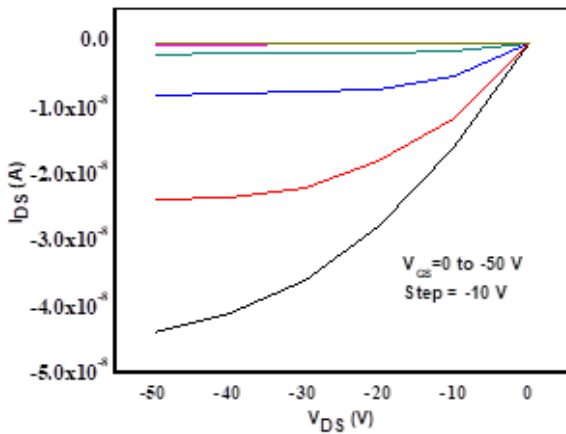


Fig.7.a. Output characteristics of CSA doped PANi-Ta₂O₅ based OFET.

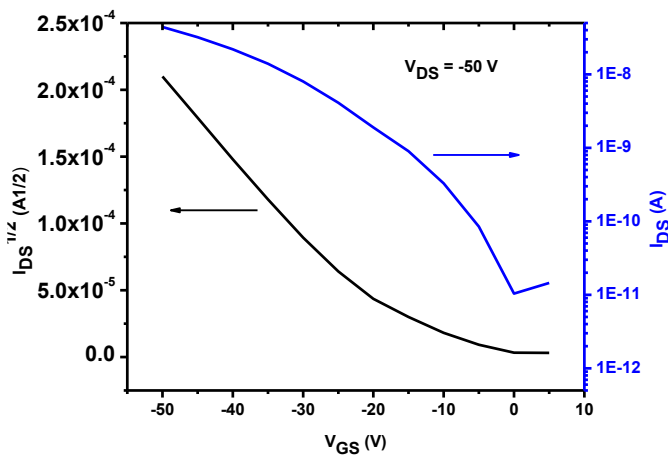


Fig.7.b. Transfer characteristics of CSA doped PANi-Ta₂O₅ based OFET.

The field-effect mobility, μ was estimated from the transfer curve in saturated regime shown in fig.6.b and the following equation:

$$I_{DS} = \frac{W}{L} \mu C_i \frac{1}{2} (V_G - V_{TH})^2 \text{ ----- (1), } V_{DS} > (V_{GS} - V_{TH})$$

where W and L are the channel width and length and C_i is the capacitance of the gate dielectric per unit area. Here, the values of these parameters are $W=1$ cm, $L=1$ mm and $C_i=6.195 \times 10^{-9}$ F/cm².

In the saturation regime, mobility was extracted from the $\sqrt{I_{DS}}$ versus V_{GS} plot by solving the following equation:

$$\mu_{sat} = \frac{2L}{WC_i} \left(\frac{\partial \sqrt{I_{DS}}}{\partial V_{GS}} \right)^2 \text{ ----- (2)}$$

The threshold voltage was obtained by extrapolating the transfer curve.

The device yielded mobility of 0.12 cm²/V-s and threshold voltage -12.89 V.

Current on/off ratio was calculated from the transfer curve again by taking I_{ON} as I_{DS} at maximum values of V_{DS} and V_{GS} . I_{OFF} is the minimum of I_{DS} at maximum value of V_{DS} . Thus, the current on/off ratio was found as $\sim 10^3$.

The sub-threshold swing, SS , was obtained from logarithmic plot of I_{DS} versus V_{GS} plot (Fig. 6.b) using equation 3. This was found to be 9.3 V/dec.

$$SS = \left(\frac{\partial \log |I_{DS}|}{\partial V_{GS}} \right)^{-1} \text{ ----- (3)}$$

The value of SS should be as low as possible because for low power applications it is crucial to have a small ∂V_{GS} that can turn the device from fully “off” to fully “on” state [44].

Electrical parameters of the CSA doped PANi-Ta₂O₅ OFET are summarized in table I.

TABLE – I

(Summary of device parameters of PANi-Ta₂O₅-CSA based OFET)

Charge Carrier Mobility (μ)	Threshold Voltage (V_{TH})	Current ON/OFF ratio (I_{ON}/I_{OFF})	Subthreshold swing (SS)
0.12 cm ² /V-s	-12.89 V	$\sim 10^3$	9.3 V/dec.

Y.R. Su et al. [44] demonstrated low-voltage operated OFETs based on copper phthalocyanine (CuPc) utilizing solution processed high-k dielectric Al₂O₃/TiO_x (ATO) and obtained values of μ , V_{TH} , current on/off ratio and SS as 0.15 cm²/V-s, -1.1 V, 5×10^3 and 232 mV/dec. respectively. The same group also devised the CuPc based OFET using low-k dielectric SiO₂ and attained less satisfactory results. The obtained μ and V_{TH} are 2.8×10^{-3} cm²/V-s and -6.0 V respectively. The device exhibited moderate current on/off ratio on the order of 10^3 and a sub-threshold swing (SS) of 5.9 V/dec.

J. Tardy et al. [45] devised pentacene based OFETs using high-k HfO₂ as the dielectric deposited using sol-gel process. They attained a high mobility of 0.12 cm²/V-s with considerable device stability.

Large values of V_{TH} and SS might be due to the existence of localized hole trapping states near the highest occupied molecular orbital and electron trapping states near the lowest unoccupied molecular orbital. This phenomenon generally happens in OFETs [46].

The relatively high charge carrier mobility of our OFET device might have resulted from the decrease in source and drain contact resistance due to the long conducting channel which leads to a weaker influence of the channel resistance [47]. Also, the highly crystalline nature of the organic semiconductor might have been a contributing factor [48]. Charge carriers are more dynamic in crystalline regions in conducting polymers due to the existence of highly ordered and stronger π - π stacking [49].

We studied the atomic force microscopy (AFM- Model No.

NTEGRA Vita from NT-MDT) imaging of the proposed device to obtain insights on the surface morphology and roughness features.

Fig. 8 shows the topographic image of the area between the source and drain contact areas of the PANi-Ta₂O₅-CSA layer deposited on the PMMA dielectric layer. The AFM image clearly shows the well defined morphology of the organic upper layer with granular microstructure. The surface of the PANi-Ta₂O₅-CSA layer was found smooth with a root mean square (rms) roughness of 0.764 nm.

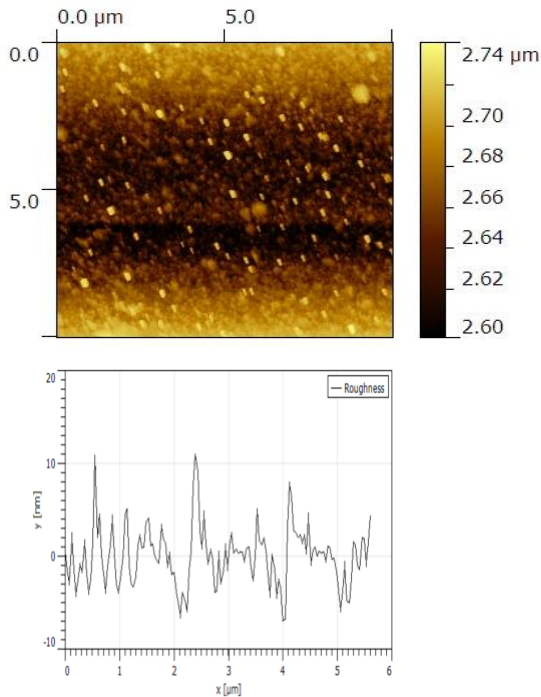


Fig. 8. AFM surface morphology of the CSA-PANi-Ta₂O₅ layer deposited on the PMMA layer (area between the source and the drain contacts) with rms roughness 0.764 nm.

It can be stated that the PMMA structure beneath the semiconductor layer might have favored the growth of the relatively smooth organic layer surface. There is high possibility of enhanced crystallinity of the CSA-PANi-Ta₂O₅ layer grown on PMMA. These factors are attributed for the improved carrier mobility of the device.

High carrier mobility results into high conductivity which in turn speeds up the charge transport in the active layer. This can facilitate an improved gas sensing feature of the semiconductor layer [50].

Although the polymeric dielectrics like PMMA have comparatively smaller value of dielectric constant, k (and hence smaller capacitance) compared to inorganic dielectrics (but higher than SiO₂), they can be easily solution processed and are compatible with flexible substrates. Thus, they can offer high-quality smooth surface helping in the proper growth of the semiconductor layer [28]. A polymeric dielectric can operate at a low processing temperature, can reduce the leakage current [30] and facilitate a trap-free semiconductor/dielectric interface enhancing the charge carrier mobility [31].

The solubility of PMMA rendered a good synergy between

the former and the organic semiconductor and, helped in a favorable growth of the active layer [51]. This facilitates an improved interface leading to supposedly low leakage current and moderately high current on/off ratio [28]. Also, PMMA being hydrophobic in nature hinders the migration of contaminants into semiconductor-dielectric interface, thus reducing the no. of charge trapping sites [52].

However, our proposed device depicted a high operating voltage and relatively high threshold voltage. PMMA possesses a low dielectric constant and hence low capacitance which can lead to high operating voltage and high threshold voltage [27]. These issues can be solved by considering the advantages of high- k oxides for low voltage and low- k polymer for high quality surface with careful blending of the two materials [53-55].

IV. Conclusion

In this study, we demonstrated OFETs based on CSA doped PANi-Ta₂O₅ nanocomposite as the active layer and PMMA as the gate dielectric. The surface morphology of the CSA doped PANi-Ta₂O₅ nanocomposite revealed highly aggregated globular structures. The AFM results revealed a relatively smooth semiconductor layer with roughness (rms) 0.764 nm. The device exhibited a good charge carrier mobility of 0.12 cm²/V-s and moderately high current on/off ratio of the order of 10³, but large operating voltage, threshold voltage and subthreshold swing. The role of PMMA as the gate dielectric and the highly crystalline nature of the CSA doped PANi-Ta₂O₅, as revealed by the XRD graphs, contributed in obtaining a relatively high charge carrier mobility of the device.

The fabrication process of the device found cost-effective and straightforward with ease of material processibility. Thanks to the high solubility of the organic semiconductor and the polymer dielectric used which enabled solution-processed fine deposition of both the layers.

It can be concluded that the use of CSA doped PANi-Ta₂O₅ nanocomposite as the active layer and PMMA as the gate dielectric leads to a viable means to develop room-temperature operable OFETs for future use, particularly in the area of gas sensing. There is further scope to improve the device performances in terms of low operating voltage, small threshold voltage and subthreshold swing by working upon a shorter channel length, hybrid dielectric, and tailoring the semiconductor/dielectric interface.

V. Acknowledgement

The authors would like to thank the Micro-Fabrication Facility unit, Department of Electronics and Communication Engineering, Tezpur University for providing cooperation and laboratory facility to carry out our research work.

References

- [1] J. Zhao, G. Wu, Y. Liu, X. Tao, W. Chen, "A wearable and highly sensitive CO sensor with a macroscopic polyaniline nanofibre membrane", *Journal of Materials Chemistry A*, Issue 48, 2015.

- [2] C. Kotlowski, P. Aspermaier, H. U. Khan, C. Reiner-Rozman, J. Brey, S. Szunerits, J. Kim, Z. Bao, C. Kleber, P. Pelosi, W. Knoll, "Electronic biosensing with flexible organic transistor devices", *Flexible and Printed electronics*, 3(2018) 034003.
- [3] K.H. Lee, J. Choi, S. Im, "Low-voltage-driven pentacene thin-film transistor with an organic-inorganic nanohybrid dielectric", *Applied Physics Letter*, 91, 123502, 2007.
- [4] X. Wu, J. Huang, "Array of Organic Field-Effect Transistor for Advanced Sensing", *IEEE Journal on Emerging and Selected Topics in Circuits and Systems*, Vol 7, Iss 1, March 2017.
- [5] M. Irimia-Vladu, E.D. Glowacki, N.S. Sariciftci, S. Bauer, "Green Materials for Electronics", *John Wiley & Sons, Technology and Engineering*, Sept, 2017
- [6] O. Knopfmacher, M.L. Hammock, A.L. Appleton, G. Schwartz, J. Mei, T. Lei, J. Pei, Z. Bao, "Highly stable organic polymer field-effect transistor sensor for selective detection in the marine environment", *Nat Commun* 5, 2954, (2014).
- [7] H. Klauk, M. Halik, U. Zschieschang, F. Eder, G. Schmid, C. Dehm, "Pentacene organic transistor and ring oscillators on glass and on flexible polymeric substrates", *Applied Physics Letter*, 82, 4175, (2003).
- [8] Y.Y. Lin, D.J. Gundlach, S.F., Neson, T.N. Jackson, "Stacked pentacene layer organic thin-film transistors with improved characteristics", *IEEE Electron Device Letters*, 18(12), 606-608, (1997).
- [9] L. N. Ismail, S. Samsul, M. Z Musa and S. Norsabrina, "Fabrication of p-type organic field effect transistor using PMMA:TiO₂ nanocomposite as the dielectric layer", *IOP Conference Series: Material Science and Engineering* 340 (2018) 012005.
- [10] K. Kim, M.K. Kim, H.S. Kang, C. Choi, "New growth method of rubrene single crystal for organic field-effect transistor", *Synthetic Metals* 157(10-12):481-484, June 2007.
- [11] Y. Li, Y. Lin, H.Yeh, T.Wen, "Ion-modulated electrical conduction in polyaniline based field-effect transistors", *Appl. Phys. Lett.* 92, 093508 (2008).
- [12] S. J. Park, C. S. Park and H. Yoon, "Chemo-Electrical Gas Sensors Based on Conducting Polymer Hybrids", *Polymers* 9(5):155, Apr 2017.
- [13] T. Le, Y.Kim, H. Yoon, "Electrical and electrochemical properties of conducting polymers", *Polymers*, review, MDPI, March 2017.
- [14] S.L. Patil, M.A. Chougule, S.G. Pawar, S. Sen, V.B. Patil, "Development of Polyaniline-ZnO nanocomposite gas sensor", *Sensors and Transducers Journal*, 34 (2011) 120-131.
- [15] J. Yakhmi, V. Saxena, D.K. Aswal, "Conducting Polymer Sensors, Actuators and Field-Effect Transistors", *Functional Material* (book), Dec 2012.
- [16] S.H. Mir, L. A. Nagahara, T. Thunder, P. Mokarian-Tabari, H. Furukawa, A. Khosla, "Review—Organic-Inorganic Hybrid Functional Materials: An Integrated Platform for Applied Technologies", *Journal of The Electrochemical Society*, 2018, Vol. 165, Iss 8.
- [17] S. Huh, H.H. Choi, K. Cho, S.B. Kim, "Photopatternable Conducting Polymer nanocomposite with incorporated gold nanoparticles for use in organic field effect transistors", *Bull. Korean Chem. Soc.*, 2012, Vol. 33, No. 4.
- [18] S. Huh, B. Chae, S.B. Kim, "Two strategies for the self-assembly of gold nanoparticles: Photoreaction and radical reaction", *Journal of Colloid and Interface Science* 327(1):211-5, Sept. 2008.
- [19] X. Chen, H. Zhang, Y. Zhang, X. Guan, Z. Zhang and D. Chen, "Low-Power Flexible Organic Field-Effect Transistors with Solution-Processable Polymer-Ceramic Nanoparticle Composite Dielectrics", *nanomaterials* 10(3):518, March 2020.
- [20] X. Guo, Y. Kang, T. Yang, S. Wang, "Low temperature NO₂ sensors based on polythiophene/WO₃ organic-inorganic hybrids", *Transactions of Nonferrous Metals Society of China*, Vol. 22, 2012
- [21] S.T. Navale, A.T. Mane, M.A. Chougule, R.D. Sakhare, S.R. Nalage, V.B. Patil, "Highly selective and sensitive room temperature NO₂ gas sensor based on polypyrrole thin films", *Synthetic Metals*, 2014
- [22] M L Rozemarie, B. Andrei, H. Liliana, R. Cramariac, O. Cramariuc "Electrospun Based Polyaniline Sensors – A Review", *IOP Conf. Material Science and Engineering*, 2017.
- [23] S.G. Pawar, S.L. Patil, R. Godase, R. N. Mulik, Shashwati Sen, and V. B. Patil, "New Method for Fabrication of CSA Doped PANi-TiO₂ Thin-Film Ammonia Sensor", *IEEE Sensors Journal*, Vol. 11, No. 11, November 2011.
- [24] B.T. Raut, M.A. Chougule, S.R. Nalage, D.S. Dalavi, Sawanta Mali, P.S. Patil, V.B. Patil, "CSA doped polyaniline/CdS organic-inorganic nanohybrid: Physical and gas sensing properties", *Ceramics International*, 2012.
- [25] S. H. Nimkar, S. B. Kondawar, P. S. More, "Polyaniline/TiO₂ thin film based Carbon Dioxide gas sensor", *International Journal of researches in Biosciences, Agriculture and Technology*, 2015.
- [26] R.K. Sonker, B.C. Yadav, A. Sharma, M. Tomar, V. Gupta, "Experimental investigations on NO₂ sensing of pure ZnO and PANI-ZnO composite thin films", *RSC Advances*, 2016.
- [27] J. Lu, K. Moon and C. P. Wong, "High-k Polymer Nanocomposites as Gate Dielectrics for Organic Electronics Applications," 2007 *Proceedings 57th Electronic Components and Technology Conference*, Reno, NV, 2007, pp. 453-457.
- [28] C. G. Alvarado-Beltrán, J. L. Almaral-Sánchez, I. Mejía, M. A. Quevedo-López, R. Ramirez-Bon, "Sol-Gel PMMA-ZrO₂ Hybrid Layers as Gate Dielectric for Low-Temperature ZnO-Based Thin-Film Transistors", *ACS Omega* 2017 2 (10), 6968-6974.
- [29] R. R. Navan, K. Prashanthi, M.S. Baghini, V.R. Rao, "Solution processed photopatternable high-k nanocomposite gate dielectric for low voltage organic field effect transistors", *Microelectronic Engineering*, vol 96, Aug. 2012.
- [30] Houin, G. J. R., Duez, F., Garcia, L., Cantatore, E., Torricelli, F., Hirsch, L. Abbas, M, "High performance low voltage organic field effect transistors on plastic substrate for amplifier circuits", *Organic Field-Effect Transistors XV, 28 August 2016*, San Diego, California (pp. 1-6), [99430H] (Proceedings of SPIE; Vol. 9943).
- [31] W. Shi, Y. Zheng, J. Yu, "Polymer dielectric in organic field effect transistor", *Properties and applications of polymer dielectric*, May, 2017, DOI: 10.5772/65916.
- [32] Puigdollers J, Voz C, Martin I, Orpella A, Vetter M, Alcubilla R, "Pentacene thin-film transistors on polymeric gate dielectric: Device fabrication and electrical characterization", *Journal of Non-Crystalline Solids* 338(1): 617-621, May 2004.
- [33] K. Amer, S. Ebrahim, M. Fateha, A.M. Elshaer, "Organic field effect transistor based on polyaniline - dodecylbenzene sulphonic acid for humidity sensor", *34th NRSC*, Feb. 2017.
- [34] C. Jung-Kubiak, A. Malaikal, A. Sidorenko, T. Siegrist, "Pentacene-based thin film transistors with titanium oxide-polystyrene/polystyrene insulator blends: High mobility on high K dielectric films", *Applied Physics Letter*, 90(6):062111-062111-2, Feb. 2007.
- [35] C. Wang, C. Hsieh, "Flexible organic thin-film transistors with silk fibroin as the gate dielectric", Apr. 2011, *Advanced Materials* 23(14) 1630-4.
- [36] J. Yang, Z. Zhao, S. Wang, Y. Guo, Y. Liu, "Insight into high-performance conjugated polymers for organic field-effect transistors", *Review, Chem*, vol. 4, iss 12, Dec 2018, 2748-2785.
- [37] D. Fichou, G. Horowitz, "Molecular and polymer semiconductors, conductors, and superconductors : overview", in *Encyclopedia of materials : Science and Technology*, 2001.
- [38] J.C. Perkinson, "Organic Field-Effect Transistors", OFET term paper, *web.mit.edu*, Nov. 2007.
- [39] B.B. Patowary, S. Laskar, R. Narzary and A. Mondal, "Synthesis, Characterization and Study of NO₂ gas sensing behavior of CSA doped PANi-Ta₂O₅ nanocomposite", *IEEE Sensors Journal*, Dec. 2019, DOI: 10.1109/JSEN.2019.2959435.
- [40] M. Harb, S. Ebrahim, M. Soliman, M. Shabana, "Fabrication of organic field effect transistor as ammonia gas sensor based on

- polyaniline channel”, International Journal of Chemical and Applied Biological Sciences, vol. 1, no. 5, 2014, p. 48, June 2020.
- [41] J.L. Huang, D. R. Hines, B. J. Jung, J. Cumings, “Polymeric semiconductor/grapheme hybrid field-effect transistors”, *Organic Electronics* 12(9):1471-1476, Sept 2011.
- [42] Y. Chu, X. Wu, J. Du, J. Huang, “Enhancement of organic field-effect transistor performance by incorporating functionalized double-walled carbon nanotubes”, *RSC Adv.*, 2017, 7, 30626.
- [43] Henry D. Tran, J.M. D’Arcy, Yue Wang, P.J. Beltramo, V. Strong and R.B. Kaner, “The Oxidation of aniline to produce “polyaniline” : a process yielding many different nanoscale structures”, *Mater. Chem.*, 2011, 21,3534– 3550 DOI: 10.1039/C0JM02699A.
- [44] Y. R. Su, W. G. Xie, Y. Li, Y. Shi, N. Zhao, J.B. Xu, “A low-temperature, solution-processed high-k dielectric for low-voltage, high performance organic field-effect transistors (OFETs)”, *J. Phys. D: Appl Phys.* 46(2013) 095105 (8pp).
- [45] J. Tardy, M. Erouel, A.L. Deman, A. Gagnaire, V. Teodorescu, M.G. Blanchin, B. Canut, A. Barau, M. Zaharescu,” Organic thin film transistors with HfO₂ high-k gate dielectric grown by anodic oxidation or deposited by sol-gel”, *Microelectronics Reliability*, vol 47, iss 2-3, 2007, pages 372-377.
- [46] T. Nagase, T. Hirose, T. Kobayashi R. Ueda, A. Otomo, H. Naito, “Influence of Substrate Modification with Dipole Monolayers on the Electrical Characteristics of Short-Channel Polymer Field-Effect Transistors”, *Applied Sciences*, Aug. 2018.
- [47] X. Wang, X. Zhang, L. Sun, K.K. Gleason, “High electrical conductivity and carrier mobility in oCVD PEDOT thin films by engineered crystallization and acid treatment”, *Science Advances* 4(9):eaat5780, Aug. 2018.
- [48] S. Y. son, Y. Kim, J. Lee, G. Lee, “High-field-effect mobility of low-crystallinity conjugated polymers with localized aggregates”, *Journal of the American Chemical Society*, 2016, 138(26), 8096-8103.
- [49] R. Li, Y. Zhou, M. Sun, Z. Gong, “Article influence of charge carriers concentration and mobility on the gas sensing behavior of tin dioxide thin films”, *Coatings* 2019, 9(9), 591.
- [50] V. P. Liyana, Stephania A M, K Shiju, P Predeep, “Influence of gate dielectrics, electrodes and channel width on OFET characteristics”, *Journal of Physics: Conference Series* 619 (2015) 012029.
- [51] M. Yi, J. Guo, W. Li, L. Xie, Q. Fan, W. Huang, “High-mobility flexible pentacene-based organic field-effect transistors with PMMA/PVP double gate insulator layers and the investigation on their mechanical flexibility and thermal stability”, *RSC advances* 5(115), Nov. 2015.
- [52] P. J. Diemer, Z. A. Lamport, Y. Mei, J. W. Ward, “Quantative analysis of the density of trap states at the semiconductor-dielectric interface in organic field-effect transistors”, *Appl. Phys. Lett.* 107, 103303 (2015).
- [53] L. Shang, M. Liu, D. Tu, G. Liu, X. Liu, and Z. Ji, “Low-Voltage Organic Field-Effect Transistor with PMMA/ZrO₂ Bilayer Dielectric”, *IEEE Transaction on electron devices*, vol 56, no.3, pp 370-376, March 2009.
- [54] A.L. Deman, J. Tardy,” PMMA-Ta₂O₅ gate dielectric for low operating voltage organic FETs”, *Organic Electronics*, vol 6, iss 2, April 2005, pages 78-84.
- [55] X. Hou, S. ChoonNg, J. Zhang, J.S. Chang, “Polymer nanocomposite dielectric based on P(VDF-TrFE)/PMMA/BaTiO₃ for TIPS-pentacene OFETs”, *Organic Electronics*, vol 17, Feb 2015, Pages 247-252.



Bornali Bora Patowary obtained her B.E degree in Electronics & Communication Engineering from Assam Engineering College, Gauhati University and M.Tech degree from NERIST, Itanagar. Earlier, she was associated with Management Information System (MIS) and Database



Management Systems in various industrial and educational organizations for more than five years. Currently, she has been working as Assistant Professor in the department of Electronics & Communication Engineering, Central Institute of Technology, Kokrajhar, Assam-783370. Her research interest includes synthesis of conducting polymers and their composites for gas sensing and OFETs.

Dr. Shakuntala Laskar is presently working as Professor and holding the position of Head Of the Department, Electrical and Electronics Engineering Department, Don Bosco College of Engineering and Technology, Assam Don Bosco University, Assam-781017. She received her bachelor degree in Electrical Engineering from Assam Engineering College, Gauhati University and M.Tech and Ph.D degrees from IIT Kharagpur. Her research interest includes electro-optics, MEMS and sensors.



Rewrewa Narzary received his B.Tech degree in Electronics and Communication Engineering from Central Institute of Technology, Kokrajhar, Assam in 2013 and M.Tech degree from Tezpur University, Assam in 2015. He is currently working towards the Ph.D. degree at Tezpur University, Assam-784028. His research interest includes semiconductor material characterization and device fabrication.